Degree of Stereochemical Control of *rac*-Et[Ind]$_2$ZrCl$_2$/MAO Catalyst and Properties of Anisotactic Polypropylenes[1]

Bernhard Rieger, X. Mu, D. T. Mallin, Marvin D. Rausch, and James C. W. Chien*

Department of Polymer Science and Engineering, Department of Chemistry, University of Massachusetts, Amherst, Massachusetts 01003

Received October 18, 1989; Revised Manuscript Received December 21, 1989

ABSTRACT: Polypropylenes had been obtained with racemic ethylenebis(indenyl)zirconium dichloride/methyl aluminoxane (MAO) catalyst from −55 to +80 °C and Al/Zr ratios between 10^3 and 1.6×10^4. As the polymerization temperature increases, the polymers produced have progressively lower melting transition temperature, lower homosteric pentad sequence population, and higher solubility in low-boiling solvents, indicating frequent stereochemical inversion in monomer enchainment. Polymer fractions separated by solvent extraction are relatively crystalline (crystallinity > 50%) favoring a thermally stable γ-modification. The ^{13}C NMR spectra also showed the presence of tetramethylene unit in acetone- and ether-soluble fractions. In addition, there is tail-to-tail enchainment in PP obtained at a low MAO to Zr ratio. The results indicate variations of degrees of stereochemical and regiochemical control by the *rac*-Et[Ind]$_2$ZrCl$_2$/MAO catalyst with polymerization temperature and catalyst composition.

Ziegler–Natta (ZN) catalysis is in a state of renaissance with new scientific discoveries and technological advances in both heterogeneous and homogeneous systems. With regard to heterogeneous systems, the classical δ-$TiCl_3$·0.33$AlCl_3$/$AlEt_2Cl$ catalyst has only a minute fraction of the Ti ions catalytically active for isospecific polymerization of propylene. The new $MgCl_2$-supported $TiCl_3$ catalysts[2,3] have 100-fold more active sites per mole of Ti[4] ([C*]), each C* having a 10 times faster rate constant of propagation (k_p), which in the presence of electron-donating promoters[5] produces polypropylene (PP) having an isotactic yield (IY) of 99% as compared to 92% by the δ-$TiCl_3$ catalyst. Here, IY is the percent of refluxing *n*-heptane-insoluble fraction which crystallizes in the α-modification and has a melting transition (T_m) of ≥165 °C.

Bis(cyclopentadienyl)titanium dichloride (Cp_2TiCl_2; Cp = η^5-cyclopentadienyl)/aluminum alkyl chloride was the first homogeneous ethylene polymerization catalyst.[6] The active tetravalent Ti complex decays rapidly by reductive elimination of polymer chains.[7] The catalyst produces only 1.2×10^4 g of polyethylene (PE)/(mol Ti·h·atm) and does not polymerize propylene. Subsequently, small amounts of water were found to increase significantly the activity of the catalyst.[8] The reaction between water and aluminum alkyls was shown to produce alkyl aluminoxanes.[9] With use of oligomeric methyl aluminoxane (MAO) as the cocatalyst,[10] Cp_2TiCl_2 polymerizes ethylene with a productivity of 10^7 g of PE/(mol Ti·h·atm) at 20 °C; the productivity is 10^8 g of PE/(mol Zr·h·atm) at 70 °C for Cp_2ZrCl_2/MAO. However, these achiral complexes produced only atactic PP.[10b,c,11] Similarly, the *meso*-Et[Ind]$_2$ZrCl$_2$[12]/MAO[13] (Et[Ind]$_2$ = ethylenebis(indenyl)) and *meso*-Et[Ind]$_2$TiCl$_2$/MAO[14] systems are also nonstereospecific.

The significant new discovery is that isotactic PP can be obtained with chiral *rac*-Et[Ind]$_2$ZrCl$_2$[13] and *rac*-Et[$IndH_4$]$_2$TiCl$_2$[14] (Et[$IndH_4$]$_2$ = ethylenebis(tetrahydroindenyl)) activated with MAO. This finding demonstrated stereochemical control by the chiral *ansa*-indenyl ligands on the transition-metal ion in the selection of one of the two enantiotopic faces (Re or Si)[15] of the prochiral propylene monomer in its migratory insertion. Other new stereospecific catalyst systems have been found: *i*-propyl(cyclopentadienyl-1-fluorenyl)hafnium dichloride/MAO[16] for syndiospecific propylene polymerization and tetrabenzyl- or tetraalkoxyltitanium/MAO[17] for syndiospecific styrene polymerization. These developments have attracted organometallic chemists to participate in this rapidly expanding research area.

ZN catalysts are not totally stereospecific because there are nonspecific sites or sites having variable stereospecificity. Even the best heterogeneous ZN catalyst produces PP, which contains 2–5% racemic diads.[18] The chiral metallocene/MAO catalysts have variable stereochemical controls as judged by the stereoregularities of the PP produced. Ewen[14] observed that the polymer obtained with *rac*-Et[$IndH_4$]$_2$$TiCl_2$ at 0 °C has methyl pentad fractions of [*mmmm*] = 0.56 and [*rrrr*] = 0.006, a total *m* placement of 86%, and a very low T_m of 99 °C. The "isotactic" PP produced at −60 °C contains 95% *m* placement and has T_m = 144 °C. Kaminsky et al.[13a] reported that the polypropylenes obtained with *rac*-Et[$IndH_4$]$_2$ZrCl$_2$/MAO between −10 and +20 °C are highly isotactic, and less than 1% of the polymer was soluble in toluene (conditions unspecified).[10a] Subsequently, Soga et al.[19] obtained polypropylene with the *S*-enantiomer of Et[$IndH_4$]$_2$ZrCl$_2$ at −10 °C and extracted the polymer with boiling *n*-heptane. The insoluble material (amount not given) has T_m = 160 °C and [*mm*] = 0.986; the soluble portion (amount also not given) has T_m = 149 °C and [*mm*] = 0.961. ^{13}C NMR spectroscopy revealed a tetramethylene sequence, which was attributed to hydrogen-transfer 1,3-insertion. Grassi et al.[20] found the stereoregularity of the PP obtained with *rac*-Et[$IndH_4$]$_2$ZrCl$_2$/MAO depended on the temperature of polymerization; the *mmmm* pentad sequence decreased from 0.95 to 0.75 for polymers obtained at 0 and 25 °C, respectively. There were also significant amounts of 1,3-insertions and head-to-head enchainment.

Natta recognized that catalysts low in stereospecificity, such as $TiCl_4/AlEt_3$, produced a mixture of polypropylenes, which differ both in molecular weight (MW) and in stereoregularity[21,22] which can be separated by solvent fractionation.[22,23] The PP obtained with the chiral metallocene/MAO systems has not been rigorously characterized in this manner.

0024-9297/90/2223-3559$02.50/0

Table I
Propylene Polymerizations by Et[Ind]$_2$ZrCl$_2$/MAO[a]

T_p, °C	A, ×10^{-3} kg of PP/[Zr][monomer]·h	T_m, °C
80	~7.8	104
70	7.67, 7.16, 7.91	107
50	4.25, 4.1	128
30	2.31, 2.0	136
20	1.26	138
0	0.14, 0.15, 0.16	143
-20	0.03, 0.026, 0.037	147
-55	0.002, 0.0027	152

[a] [Al]/[Zr] = 2500.

The central purpose of this study is to polymerize propylene with the *rac*-Et[Ind]$_2$ZrCl$_2$/MAO catalyst over a broad range of polymerization temperatures (T_p) and catalyst composition (Al/Zr ratios), to fractionate the polymers by solvent extraction, and to characterize the fractions by X-ray, ^{13}C NMR, and DSC. We report here that the polymers soluble in low-boiling solvents, referred to as "anisotactic" PP,[24] have lower T_m, microisotacticity, and a tendency toward crystallization in a thermally stable γ-modification. The results suggest that the ansa-bridged ligand is relatively stereorigid at low temperature but is fluxional at high temperatures.

Experimental Section

rac-Et[Ind]$_2$ZrCl$_2$ was prepared according to published method.[12a] It has the same ^{1}H NMR purity as a sample of the compound obtained from Kaminsky. MAO was synthesized by an improved method of Kaminsky and Hähnsen[25] as communicated to us by Kaminsky. Purification of monomer and solvent and the polymerization procedures have been described previously.[26] Polypropylene was precipitated from the reaction mixture by a large volume of acidic methanol. The filtrate was evaporated to dryness, washed with methanol, and combined with the precipitated polymer. Polymers were fractionated by the procedure of Natta and co-workers[22,27] using solvents in the order of increasing rank: acetone (A), diethyl ether (E), *n*-pentane (C_5), *n*-hexane (C_6), and *n*-heptane (C_7).

NMR spectra were obtained with Varian 200- and 300-MHz spectrometers. Melting and crystallization curves were recorded with a Perkin-Elmer DSC IV system. A Siemens D-500 diffractometer was used to obtain powder patterns by using a Ni-filtered Cu Kα X-ray beam excited at 40 kV. All attempts to prepare an oriented fiber from PP fractions give samples having very small crystallite sizes and weak diffraction patterns.

Results

Polymerization. Polymerization of propylene was carried out in 95 mL of toluene at temperatures from -55 to +80 °C with a monomer pressure of 1.5 atm and was initiated by 9 × 10^{-6} M of *rac*-Et[Ind]$_2$ZrCl$_2$ and 2.25 × 10^{-2} M of MAO based on [Al]. The [MAO] is given in terms of Al concentration because the MW of MAO is not known with certainty and it can vary with the method of synthesis. Polymerizations were also performed at higher and lower [MAO].

The polymerization rate increases with the increase of T_p. The polymerization activity of the catalyst is given by

$$A = \frac{\text{kilograms of PP}}{\text{[Zr][monomer]·hour}} \quad (1)$$

The variation of A with T_p is summarized in Table I. Kaminsky[13] reported that the catalytic activity reached a maximum at T_p = 45 °C, above which temperature it decreases with a further increase in temperature contrary to our observation. This is because the author expressed activity in kilograms of PP per mole of Zr per hour at the pressure of monomer used without correcting for the negative temperature dependence of solubility of propylene in toluene[28] as shown in Figure 1. Samples of Et[Ind]$_2$ZrCl$_2$ given to us by Professor Kaminsky and samples synthesized in our laboratory have identical polymerization behaviors.

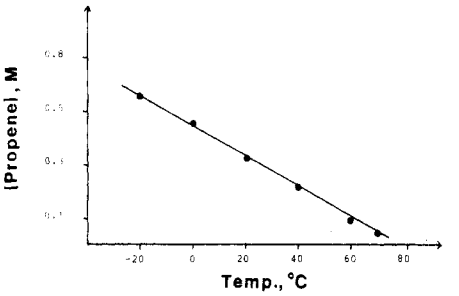

Figure 1. Solubility of propylene in toluene as a function of temperature.

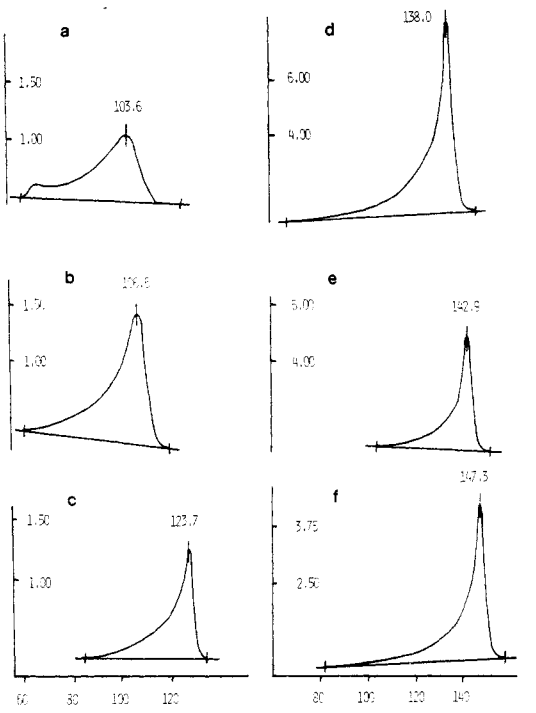

Figure 2. DSC of the total polymers at 20 °C/min heating rate; second scan after complete melting and cooling for polymers obtained at T_p: (a) 80; (b) 70; (c) 50; (d) 20; (e) 0; (f) -20 °C.

Properties of the Total Polymers. The total polymers have very broad melting DSC curves as shown in Figure 2; the T_m values are given in Table I. There is a gradual and linear decrease of T_m with T_p up to 20 °C, above which T_m drops rapidly with a further increase of T_p (Figure 3). The polymer obtained at T_p = 80 °C displays a secondary maximum in its melting endotherm (Figure 2a).

The intrinsic viscosities of the total polymers were determined and given in Table II. Their GPC curves (Figure 4) showed a steady increase of MW and narrowing of distribution as T_p decreases. The values of $\bar{M}_n$, $\bar{M}_w$, and MWD = $\bar{M}_w/\bar{M}_n$ are summarized in Table II. The MWD increases with the increase of T_p, indicating the catalytic species and/or their activities become progressively nonuniform. Various metallocene catalysts exhibit different MWD–temperature dependences. In the case of the Et[IndH$_4$]$_2$ZrCl$_2$/MAO system,[13] the value of MWD decreases from 2.6 to 1.8 as T_p increases from -10 to +20 °C. The MWD is ≤1.9 independent of T_p for polymers obtained with the Cp$_2$Ti(Ph)$_2$/MAO catalyst.[29]

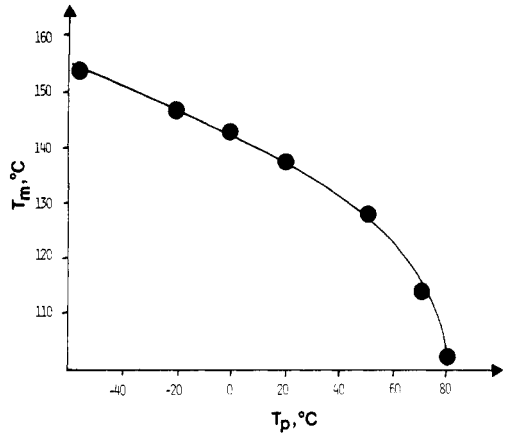

Figure 3. Variation of T_m of the total polymer with T_p of polymerization.

Since the anisotactic PP is believed to differ structurally from isotactic PP, the validity of using polystyrene standards in obtaining the MW's by GPC needs to be ascertained. Therefore, we performed light-scattering measurements on two PP samples; Figure 5 gives the Zimm plots. The $\bar{M}_w$ values thus obtained agree within ±3% with the $\bar{M}_w$ values calculated from the GPC curves (Table II, columns 4 and 8). The two PP samples have R_z values of 440 and 344 Å as expected for its $MW^{1/2}$ dependence.

The microstructures of the total polymers were determined by ^{13}C NMR. Table III summarizes the steric diad, triad, and pentad distributions of polymers obtained at different T_ps. The populations of m^n sequences (n = 1, 2, 4) all increase with the decrease of T_p. Figure 6 shows only gradual change of *mmmm* fractions from 0.86 to 0.81 between T_p of −55 to +50 °C. However, further increase of T_p resulted in a precipitous drop of [*mmmm*] to 0.41 for T_p = 80 °C.

Fractionation of Polypropylenes. The amount of polymer soluble in different solvents up to *n*-heptane and the amount of insoluble polymers are summarized in Table IV. There are no C_7-insoluble products in 70 and 80 °C polymerizations or IY = 0 in these cases. In fact, all the polymers produced in these experiments were soluble in C_6. The polymers obtained at T_p = 50 °C have IY = 17.5%. Even in the −55 °C polymerization, the IY of the product is only 86.2%. Most of the polymer fractions extracted with acetone or ether were brittle waxy substances characteristic for low-melting and low X_c (=percent crystallinity) polymers.

Properties of the Polymer Fractions. Because of the large number of samples involved, they are designated with T_p followed by the solvent that is soluble to facilitate identification. For instance, the sample 20/E refers to the ether-soluble fraction of the polymer obtained in a 20 °C polymerization; this fraction is insoluble in the next lower ranking solvent, which is acetone.

The melting transitions of the polypropylene fractions had been obtained. Figure 7 gives the DSC curves of the fractions from −55 °C polymerization; they are relatively symmetrical and sharp. In contrast, the DSC curves of the fractions from 70 °C polymerization (Figure 8) are broader and more asymmetric. In fact, the acetone and ether fractions have bimodal DSC curves (parts a and b of Figure 8, respectively) and T_m values as low as 54 °C. Table V summarizes the DSC results. The T_m values for the C_{7i} fractions, which are the refluxing *n*-heptane-insoluble polymer, are a few degrees higher than that for the total polymer; the values for the other fractions decrease with the decreasing rank of the solvent.

The effect of heating rate on the melting endotherm and the effect of cooling rate on the crystallization exotherm were investigated for the 70/C_6 fraction. In the former measurements, the polymer sample was first heated to 150 °C and cooled at 100 °C/min to room temperature, and then a second DSC curve was recorded at heating rates of 2.5, 5, 10, 20, and 40 °C/min. The same T_m of 118.5 ± 0.5 °C was obtained as shown in Figure 9, and the enthalpy of melting was constant within ±0.5 cal/g. For the second measurements, samples heated twice to 150 °C were cooled at different rates to observe the exotherm. The crystallization temperature was found to be reproducible at 101.3, 98.1, 95.4, 90.6, and 84.0 °C for cooling rates of −2.5, −5.0, −10, −20, and −40 °C/min, respectively, indicating the polymer crystallizes very slowly.

The microstructures of the polymer fractions have been determined by ^{13}C NMR, and the steric sequence distributions are summarized in Table VI. The extensive ^{13}C NMR results, the statistical analysis, and the mechanistic implications will be published elsewhere. For the 70 °C polymerization the fractions in the order of increasing solvent ranking show regular increases in the *mmmm* and *mmmr* pentads and regular decreases in the pentads having two or more *r* placements. The same holds ture for all but the −55/E fraction. The polymers obtained at 0 °C have occasional reversals in the progressions of steric sequence distributions with respect to the solvent ranking. However, none of the fractions are "atactic" according to the conventional criteria.[24]

Infrared spectra were recorded for all the anisotactic PP fractions.[30] The absorption bands at 841, 973, and 998 cm^{-1} have ratios of A_{998}/A_{973} and A_{841}/A_{973}, which bear a linear relationship to ^{13}C NMR determined [*mmmm*] with limits of unity for these ratios at [*mmmm*] = 1.

Highly isotactic PP crystallizes in the α-modification;[31] less stereoregular polypropylenes can also crystallize in the β-[31,32] and γ-modifications.[31,33] Powder X-ray diffraction patterns have been obtained for several anisotactic PP fractionations.

Polymer fractions precipitated from solution gave poor X-ray patterns and similarly for samples quenched from melt. We found it necessary to heat the specimens to above T_m and cooled them slowly over 24 h to room temperature in order to obtain sharp diffraction patterns, though it is not necessary to do the same in DSC measurements (vide supra). There are no β-phase reflections in any of the PP fractions; all the patterns are combinations of reflections from the α- and γ-modifications. The two most characteristic reflections have 2θ = 18.3° and 20° for the α- and γ-phase, respectively, which are marked accordingly in Figure 10. The percent crystallinity (X_c) was calculated by the usual method. The percent of γ-modification (C_γ) was estimated from an empirical relation[31c]

$$C_\gamma = \frac{h_\gamma}{h_\alpha + h_\gamma} \times 100 \qquad (2)$$

where h_α and h_γ are the height of the two peaks located at 2θ = 18.3° and 20°, respectively. The results are summarized in Table VII.

All the PP fractions examined have X_c lying between 54% and 68%, which increases with the order of solvent ranking and decreasing T_p. The −55/C_{7i} fraction has the same X_c as the PP obtained with an $MgCl_2$-supported $TiCl_3$ catalyst. The polymer obtained at 0 °C has both lower X_c and stereoregularity than the other samples. Except for the C_{7i} fractions, all the other fractions crystallize either significantly or predominantly in the γ-modification.

Table II
Molecular Weight Data for the Total Polymers Obtained with the Et[Ind]$_2$ZrCl$_2$/MAO System at Different Temperatures

		GPC			light scattering		
T_p, °C	[η], dL/g	$\bar{M}_n \times 10^{-4}$	$\bar{M}_w \times 10^{-4}$	$\bar{M}_w/\bar{M}_n$	A_2, $\times 10^4$ mol·cm^3·g^{-2}	R_z, Å	$\bar{M}_w \times 10^{-4}$
80	~0.1	0.86	2.32	2.69			
70	0.15	1.20	2.79	2.34			
50	0.20	1.57	4.27	2.72			
30		3.56	7.09	2.11			
20	0.58	4.76	9.44	1.98	10.5	344	8.86
0	0.74	8.96	11.6	1.30	10.1	440	12.3
-20	0.92	9.35	14.2	1.52			

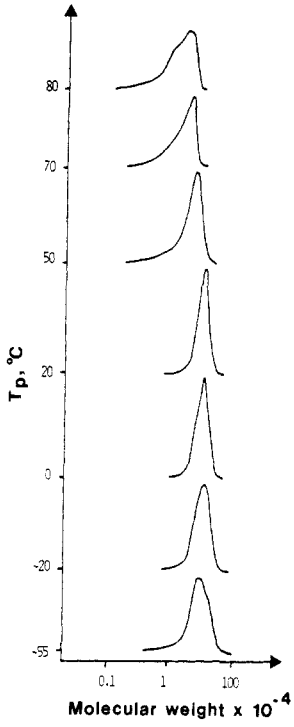

Figure 4. GPC curves for the total polymers produced at various temperatures. T_p from top to bottom: 80, 70, 50, 20, 0, -20, and -55 °C.

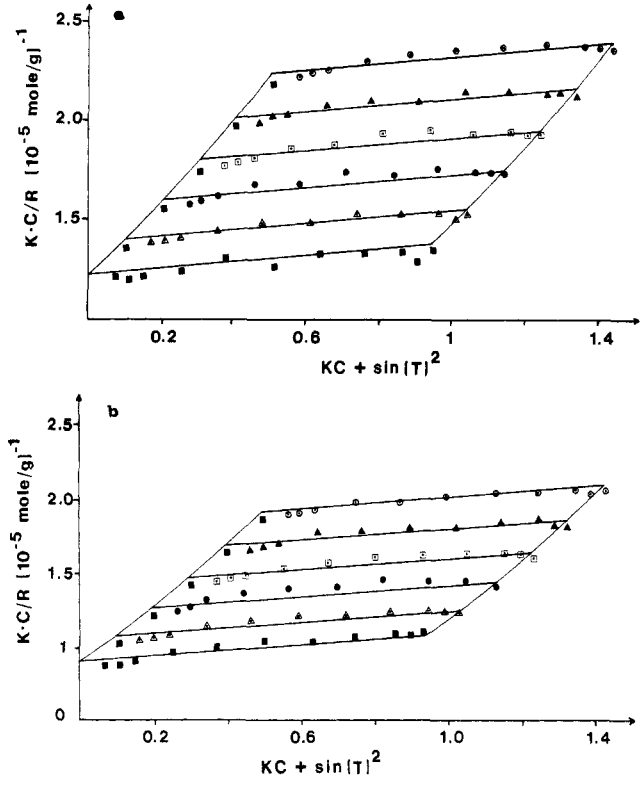

Figure 5. Zimm plots for light-scattering determinations of $\bar{M}_w$ for the total polymers obtained at (a) 20 and (b) 0 °C.

Effect of MAO Concentration. The effect of MAO on the polymerization and the structures of the polypropylenes were studied. The results on activity, T_m, and MW are given in Table VIII. The catalytic activity increases with the increase of Al/Zr. There is a linear variation of $\bar{M}_n$ versus the Al/Zr ratio, but $\bar{M}_w$ is independent of it. Consequently, the MWD is narrower at higher Al/Zr ratio; however, the curves showed no bimodality as they can be in view of the broad T_m endotherms. The polymers obtained with different Al/Zr ratios have similar T_m and distributions of homosteric sequences, but see below on structural irregularities.

Structural Irregularities. NMR is useful not only in the determination of steric sequence distributions (vide supra) but also in the detection of end groups and structural defects such as regiochemical insertion errors if they are present in amounts greater than 1%. The methyl ^{13}C NMR spectra of the polymer fractions of C_5 or higher ranking solvents have no detectable amounts of irregular resonances. However, they were observed in the A and E fractions as shown in Figure 11. Additional irregular peaks were seen in the NMR of the total polymers obtained at low Al/Zr = 10^3 (Figure 12).

Discussion

Polymerization Kinetics. With most ZN catalysts their polymerization activity as a function of T_p first increases with increasing T_p, reaching a maximum, and then decreases with a further increase in temperature. This was interpreted as slow chain initiation at low temperature and rapid catalyst deactivation at elevated temperatures.[34]

The Et[Ind]$_2$ZrCl$_2$/MAO catalyst is unusual in that the polymerization activity increases about 3000-fold from -55 to +70 °C. In fact, the Arrhenius plot (Figure 13) is linear for the entire temperature range. This gives a value of 10 kcal mol^{-1} for the overall activation energy for polymerization. This behavior indicates a very low activation energy for initiation and that there is no significant catalyst deactivation. Therefore, the activation energy for propagation is ca. 10 kcal mol^{-1}, which is very close to that for ethylene polymerization by Cp$_2$TiCl$_2$/AlMe$_2$Cl[7] and that for propylene polymerization by MgCl$_2$-supported TiCl$_4$,[4b,c] and by α-TiCl$_3$/AlEt$_2$Cl.[35] In the absence of catalyst deactivation, the number-average degree of polymerization ($\overline{DP}$) should be given by

$$(\overline{DP})^{-1} \sim R_{tr}/R_p \quad (3)$$

The rate of chain transfer, R_{tr}, is the sum of all the transfer processes. The dominant processes are the spontaneous β-hydrogen transfer and transfer to MAO. Figure 14 is an Arrhenius plot of log $\bar{M}_n$ versus T^{-1}; the slope gives $(E_{tr} - E_p)/2.303R$ and $E_{tr} \sim 15$ kcal mol^{-1}. This activation

Table III
Comparison of Observed and Calculated Steric Sequence Distributions for the Total Polymers

T_p, °C	parameters			triad				pentad									
							APD,[b]	*mrmm*									APD,
	b	*w*	model[a]	*mm*	*mr*	*rr*	%	*mmmm*	*mmmr*	*rmmr*	*mmrr*	*rmrr*	*mrmr*	*rrrr*	*mrrr*	*mrrm*	%
80			Ob	0.61	0.24	0.15		0.41	0.16	0.046	0.11	0.086	0.04	0.037	0.04	0.074	
	0.837		E	0.65	0.23	0.12	11	0.41	0.15	0.013	0.15	0.054	0.03	0.013	0.03	0.076	39
70			Ob	0.73	0.16	0.11		0.57	0.14	0.02	0.10	0.034	0.021	0.018	0.023	0.073	
	0.894		E	0.72	0.19	0.10	9	0.57	0.13	0.01	0.14	0.036	0.018	0.009	0.017	0.068	26
50			Ob	0.91	0.053	0.035		0.81	0.079	0.025	0.041	0.009	0.003	0.006	0.001	0.028	
	0.959		E	0.88	0.079	0.039	18	0.81	0.069	0.002	0.069	0.006	0.003	0.002	0.003	0.035	56
	0.97	0.005	E/C	0.91	0.06	0.03	9	0.85	0.053	0.001	0.053	0.004	0.002	0.001	0.002	0.089	76
0			Ob	0.91	0.061	0.024		0.83	0.054	0.027	0.034	0.013	0.014	0.006	0.007	0.014	
	0.964		E	0.90	0.069	0.035	17	0.83	0.062	0.001	0.062	0.005	0.002	0.001	0.002	0.031	103
	0.98	0.04	E/C	0.91	0.058	0.029	8	0.87	0.04	0.003	0.04	0.011	0.006	0.003	0.006	0.02	45

[a] Models are E (enantiomorphic – site control) and E/C (C = chain-end control), distributions calculated using equations of Ewen[28] and Dor,[44] respectively. Ob is the experimentally found distribution. [b] Average of the percentage deviation from the mean value.

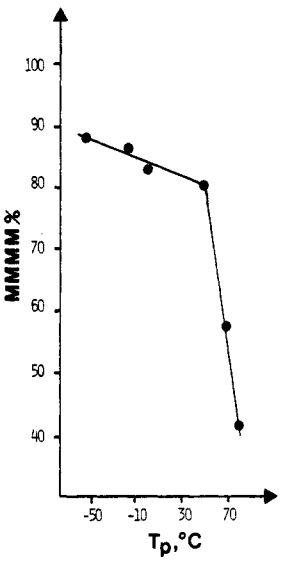

Figure 6. Variation of the steric *mmmm* pentad sequence fraction with polymerization temperatures.

Table IV
Fractionation of Anisotactic Polypropylenes by Solvent Extraction

T_p, °C	wt % of polymer soluble in					wt % of refluxing heptane insoluble
	acetone	ether	pentane	hexane	heptane	
80	22.5	34.8	17.5	25.2	0	0
70	16.4	32.0	15.3	36.3	0	0
50	6.5	13.6	2.4	46.4	13.6	17.5
20	2.4	4.7	2.8	2.6	12.9	74.6
0	2.1	4.3	2.4	2.9	13.9	74.4
-20	1.8	4.2	2.2	3.0	13.5	75.3
-55	0.2	0.9	0.4	3.1	9.2	86.2

energy is probably that required for β-hydride transfer (vide infra). The MW is only weakly dependent on T_p at low temperatures, suggesting other transfer mechanisms prevail below 0 °C which have activation energies comparable to E_p.

Morphology. The anisotropic PPs of this work are characterized by low and broad T_m, indicating microstructural heterogeneity. To understand the structures of these PP, it is absolutely essential to separate the total polymer by solvents into fractions according to microstructures. Better separation methods are available now, such as temperature rise elution fractionation (TREF), but instrumentation for TREF is not yet available in our laboratory.

The lower ranking fractions of PP obtained in 70 °C polymerization have T_m and [*m*] diads which are very similar to the most stereoregular PP obtained with the $Cp_2Ti(Ph)_2$/MAO system.[14,29] In the former, the A and E fractions have T_m ([*m*]) values of 54 °C ([0.735]) and 86 °C ([0.80]), respectively. The samples obtained with the latter system at −30 and −60 °C have T_m ([*m*]) values of 55 °C ([0.83]) and 62 °C (0.85), respectively. Ewen[14] also reported that the PP obtained with *rac*-Et[IndH$_4$]$_2$-TiCl$_2$/MAO at 0 °C has T_m = 99 °C and [*mmmm*] = 0.56.

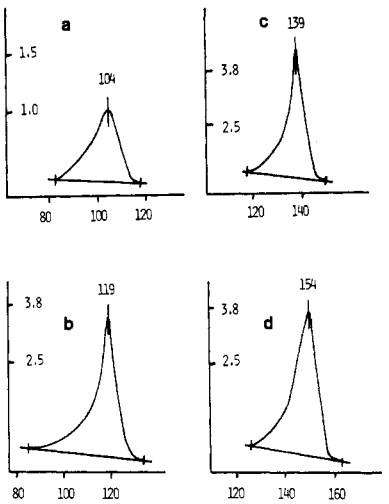

Figure 7. DSC of fractionated samples of polypropylenes obtained in −55 °C polymerization: (a) C_5; (b) C_6; (c) C_7; (d) C_{7i}. Heating rate = 20 °C/min; the *x* axis is temperature in degrees Celsius; the *y* axis is millicalories per second.

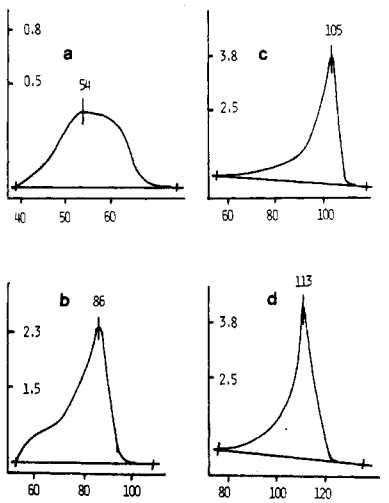

Figure 8. DSC of fractionated samples of polypropylenes obtained in 70 °C polymerization: (a) A; (b) E; (c) C_5; (d) C_6. Other remarks are the same as in Figure 7.

Table V
Melting Transition for Anisotactic Polypropylene Fractions

T_p, °C	T_m, °C: fractions soluble in acetone	ether	pentane	hexane	heptane	C_{7i} fraction	total polymers
70	54	86	105	113			107
50	wax	wax	wax	124	130	135	128
0	wax	wax	94	116	140	144	143
-20	wax	wax	wax	123	138	149	147
-55	wax	wax	104	119	139	154	152

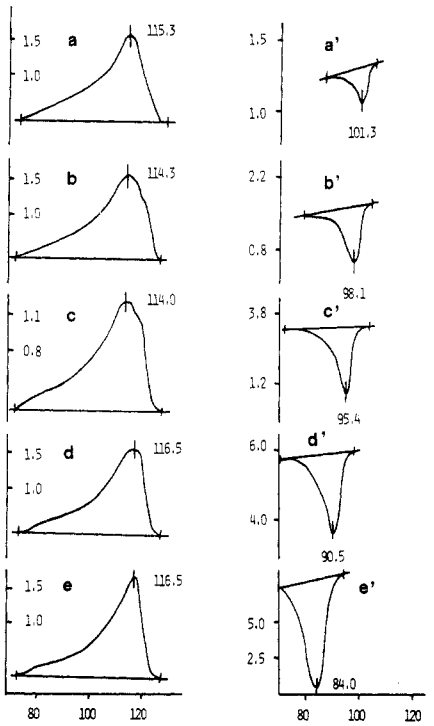

Figure 9. Effect of heating rate on the melting endotherm: (a) 2.5, (b) 5; (c) 10; (d) 20; (e) 40 °C/min. Effect of cooling rate on the crystallization exotherm: (a') -2.5; (b') -5; (c') -10; (d') -20; (e') -40 °C/min.

This is very close to the total PP obtained with *rac*-Et-[Ind]$_2$ZrCl$_2$/MAO at 70 °C, which has T_m = 107 °C (Table V) and [*mmmm*] = 0.57 (Table III).

It is reasonable to expect a correlation between T_m and the isotacticity of PP. We found that they are related by Flory's theory of melting point suppression[36]

$$\frac{1}{T_m} - \frac{1}{T_m^\circ} = -\left(\frac{R}{\Delta H_\mu}\right) \ln p \qquad (4)$$

where T_m° is the melting temperature for the perfectly regular polymer taken to be 184 °C[37] and p is the probability for a given stereounit. Figure 15 is a plot of $(1/T_m) - (1/T_m^\circ)$ versus log [*mmmm*]. Most of the data fit the given line; however, the C_5 and C_6 fractions of 0 °C polymerization do not. From the slope of the plot, one can calculate ΔH_μ = 2.7 kcal mol^{-1} in agreement with the literature values of 2.6[37] and 2.3 kcal mol^{-1}.[38]

Crystalline Morphology. The anisotactic PP fractions all exhibit preference toward γ-crystalline form. The γ-modification had been previously observed for low MW PP obtained by thermal degradation,[33d] and γ-irradiation,[33f] or by special synthesis[33e] or extracted from commercial materials.[33a,b] The polymers were usually crystallized under pressure.[33a,c] However, the γ-phases thus obtained in these materials are unstable and readily undergo crystal–crystal transition to the α-phase upon heating. The rate of this transformation had been found to depend on both the temperature and the heating rate.[33c] For instance, the DSC thermograms of low MW PP obtained at slow heating rates ≤5 °C/min have only a single high T_m for the melting of the α-phase, which indicates that the rate of γ- to α-transformation is faster than the heating rate. Melting endotherms for both γ- and α-phases were observed at 10 °C/min, whereas a single endotherm at intermediate temperature was seen at higher heating rates. Once the polymer sample is heated above 160 °C and cooled, no γ-phase remained. A subsequent DSC scan exhibits only the α-phase melting.

The γ-morphology of the anisotactic PP obtained with the chiral metallocene/MAO catalyst differs from the previous materials described above in several important respects. First, there is no α-phase endotherm at ca. 165 °C using any heating rate in DSC measurement. This indicates the absence of γ → α crystal–crystal transitions and of an appreciable amount of α-phase. Second, the γ-modification of the present anisotactic PP reformed from the melt simply by cooling at any rate without the aid of pressure. The crystallinity of the anisotactic PP fractions are more than 54% even for the low T_m samples. In contrast, the low melting fractions of PP obtained with the classical ZN catalysts have a lower degree of crystallinity by comparison as shown in Table IX. Finally, the PPs previously reported to crystallize in the γ-modification without applied pressure are very low in MW; the $\bar{M}_n$ values are 2600 for thermally degraded PP[33d] and 740–3900 by special synthesis.[33e] The anisotactic fractions have $\bar{M}_n$ ranging from 9000 to 90 000. Therefore, their preference for the γ-modification may not be attributed to low MW alone.

Let us consider various chain configurational reasons for the crystallization of the anisotactic PP in the thermally stable γ-modification. We can rule out chains having blocks of isotactic and syndiotactic conformations, because all the fractions contain [*rrrr*] ≤ 0.05. There are two main types of configurational irregularities resulting from stereochemical insertion errors. It has been shown that the most common type in PP obtained with the heterogeneous ZN catalysts is the one with the *rr* triad flanked by *m* sequences on both sides.[29,39] These PPs crystallize either in the α-modification or in the metastable γ-modification (vide supra). This leaves the other main type of configurational irregularity having a single *r* diad flanked by *m* sequences on either side. This could result if a stereochemical error is not immediately corrected, but the new configuration is maintained in the subsequent propagation events until the next insertion error occurs. In this case there is a change of helical configuration and alternation of its direction. For a single chain, the change from clockwise helix to counterclockwise helix can be realized with a low-energy barrier through a conformation close to TT.[39] Schematically the macromolecule may be written as

T|G$^+$T|G$^+$T|G$^+$T|G$^+$T|G$^+$T|TG$^-$|TG$^-$|TG$^-$|TG$^-$|TG$^-$|TG$^-$
left-handed helix inversion right-handed helix

Table VI
Steric Sequence Distributions of Polymer Fractions

T_p, °C	fraction soluble in	diad	triad fraction			pentad fraction								
		m, %	mm	mr	rr	mmmm	mmmr	rmmr	mmrr	mrmm + rmrr	mrmr	rrrr	mrrr	mrrm
70	A	73.5	0.62	0.22	0.15	0.34	0.15	0.13	0.12	0.06	0.04	0.04	0.05	0.06
70	E	80.0	0.72	0.17	0.11	0.52	0.15	0.053	0.043	0.053	0.026	0.026	0.003	0.053
70	C_5	86.2	0.79	0.15	0.065	0.62	0.13	0.04	0.092	0.046	0.007	0.009	0.01	0.046
70	C_6	88.5	0.84	0.10	0.065	0.67	0.14	0.003	0.066	0.027	0.005	0.004	0.007	0.055
0	E	63.0	0.47	0.33	0.20	0.26	0.16	0.05	0.15	0.13	0.052	0.052	0.074	0.078
0	C_5	72.0	0.57	0.28	0.14	0.38	0.175	0.058	0.13	0.067	0.042	0.025	0.067	0.059
3	C_6	83.0	0.73	0.20	0.074	0.51	0.17	0.052	0.13	0.052	0.017	0.013	0.009	0.052
0	C_7	92.0	0.89	0.067	0.033	0.82	0.044	0.027	0.049	0.011	0.007	0.005	0.012	0.016
0	C_{7i}	96.0	0.94	0.044	0.015	0.89	0.036	0.018	0.029	0.008	0.007	0.002	0.002	0.011
−55	E	66.0	0.52	0.28	0.20	0.31	0.15	0.063	0.143	0.098	0.04	0.07	0.063	0.071
−55	C_5	88.0	0.81	0.15	0.049	0.66	0.13	0.02	0.11	0.03	0.01	0.005	0.01	0.029
−55	C_6	91.0	0.86	0.10	0.044	0.77	0.064	0.027	0.062	0.032	0.003	0.007	0.003	0.034
−55	C_7	94.0	0.90	0.069	0.027	0.79	0.094	0.016	0.041	0.024	0.004	0.001	0.006	0.02
−55	C_{7i}	96.5	0.95	0.028	0.02	0.92	0.023	0.008	0.023	0.004	0.001	0.007	0.001	0.012

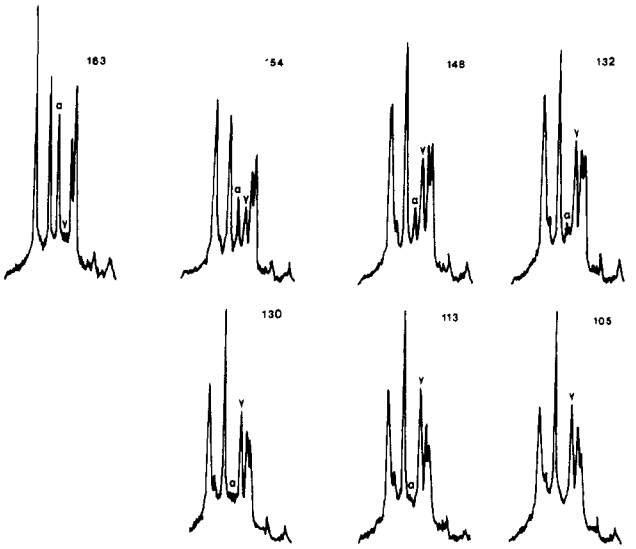

Figure 10. Powder X-ray diffraction patterns for samples of: (a) the total polymers produced with a heterogeneous ZN catalyst, T_m = 163 °C; (b) −55/C_{7i} fraction, T_m = 154 °C; (c) 0/C_{7i} fraction, T_m = 144 °C; (d) −55/C_7 fraction, T_m = 132 °C; (e) 0/C_7 fraction, T_m = 130 °C; (f) 70/C_6 fraction, T_m = 113 °C; (g) 70/C_5 fraction, T_m = 105 °C.

Table VII
X-ray Diffraction Results on Anisotactic Polypropylene Fractions

sample	X_c, %	C_γ, %
heterogeneous catalyst	68.2	8
−55/C_{7i}	68.3	42
0/C_{7i}	67.9	70
−55/C_7	65.2	87
0/C_7	48.1	89
70/C_6	59.2	93
70/C_5	54.4	100

Natta and Corradini[31] had suggested that the γ-modification becomes the preferred crystalline form if there is discontinuity in helix configuration. The anisotactic PPs produced by the Et[Ind]$_2$ZrCl_2/MAO catalyst behave as predicted by Natta and Corradini.

Regiochemical and Other Insertion Errors. In the NMR spectra of the 0/E and 70/A fractions (Figure 11), there were additional resonances. The peaks numbered 4–7 can be identified[11] with the carbon atoms in the *n*-propyl and vinylidene chain end groups.

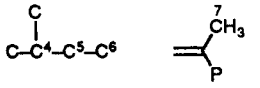

Table VIII
Polymerization Productivity and Some Polymer Properties Obtained with Different Al/Zr Ratios[a]

Al/Zr	A, ×10⁻³ kg of PP/[Zr][C_3H_6]·h	T_m, °C	[η], dL/g	$\bar{M}_n$ × 10⁻⁴	$\bar{M}_w$ × 10⁻⁴	MWD
1.1 × 10³	1.88	135.5	0.40	3.29	7.35	2.3
2.5 × 10³	2.31, 2.0	135.5, 130.1	0.36	3.36	7.09	2.1
16.4 × 10³	7.61	135.8	0.39	4.80	7.31	1.5

[a] [Zr] = 10⁻⁵ M, T_p = 30 °C.

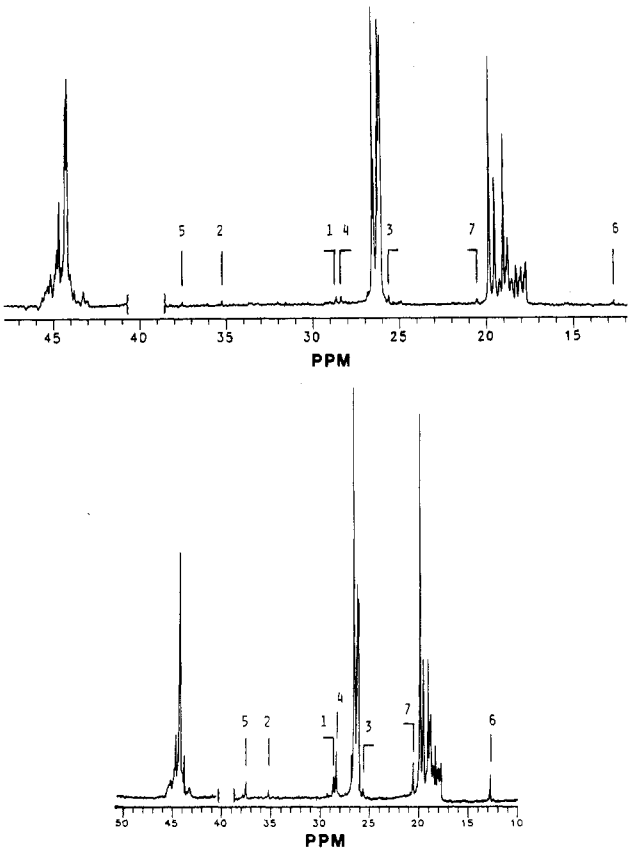

Figure 11. Methyl region NMR spectra of (a) 0/E and (b) 70/A fractions.

They are both produced by β-hydrogen chain-transfer processes

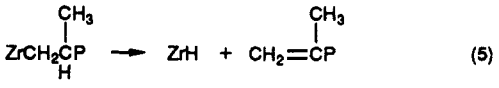

(5)

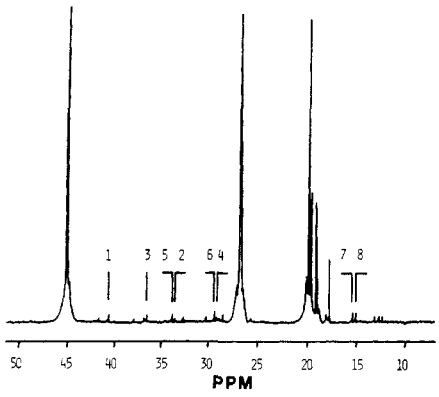

Figure 12. Methyl region NMR spectra of the total polymers obtained at 30 °C and Al/Zr = 10^3.

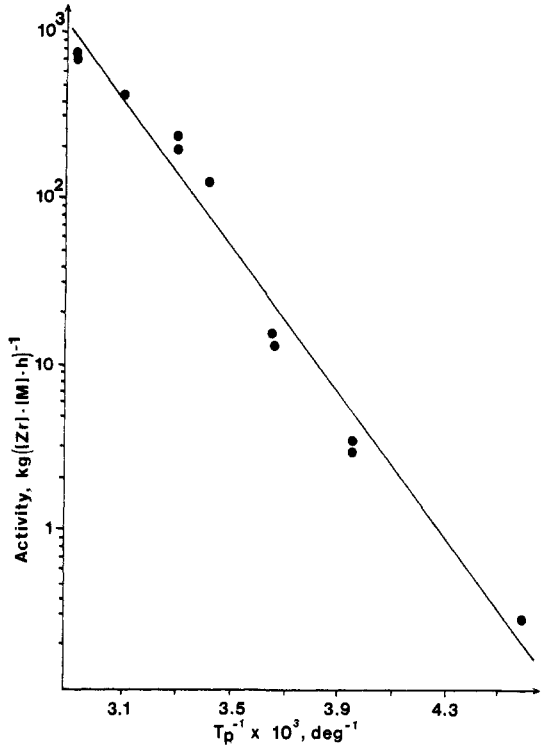

Figure 13. Arrhenius plot of polymerization activity.

where P is the polymer chain, to form the vinylidene end group. This is followed by propagation to produce the propyl end group.

$$ZrH + C_3H_6 \rightarrow ZrCH_2CH_2CH_3 \quad (6)$$

The remaining peaks 1–3 had been observed earlier.[19,20] Soga et al.[19] proposed a hydrogen transfer insertion in which the propylene is incorporated in a direct "1,3-enchainment". This process, which requires a hydrogen atom from the methyl group to be transferred to the central carbon atom of the propylene unit, is difficult to envisualize. Scheme I is proposed instead. The normal 1,2-insertion sequence (I) is interrupted by a regiochemical error of 2,1-insertion. The resulting species (II) has significantly lower reactivity toward monomer insertion, estimated to be ca. 80-fold smaller than that for the normal propagating chain (I),[40] thus permitting β-hydride elimination to occur. If the hydrogen comes from the methyl group, a terminal olefin is produced. It is depicted to remain in the coordination sphere of the metal (species III in Scheme I). The 1,2-insertion of this polymeric olefin into the zirconium hydride bond should be a very facile process.[13a] One more normal primary 1,2-insertion of the monomer into IV resulted in the observed tetramethylene sequence (V). The alternative β-hydrogen elimination

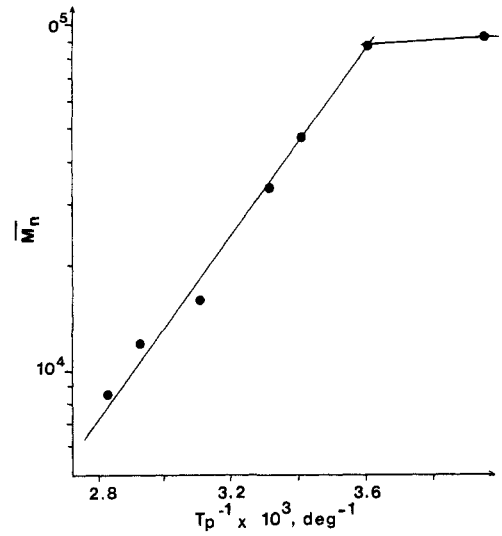

Figure 14. Arrhenius plot of $\bar{M}_n$ versus T^{-1}.

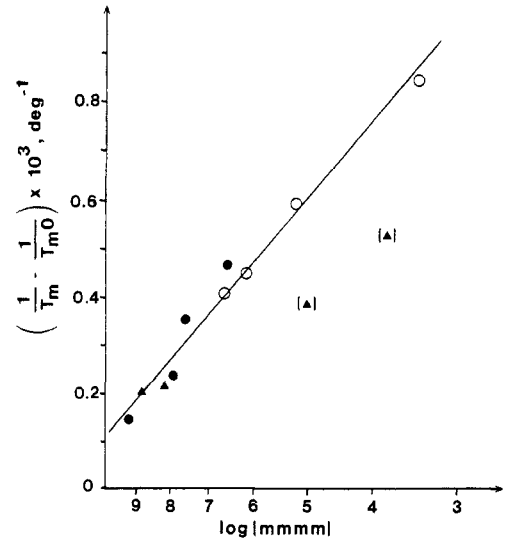

Figure 15. Plot of $(1/T_m) - (1/T_m^\circ)$ versus log [*mmmm*] for fractions of anisotactic polypropylenes: (○) T_p = 70 °C; (●) T_p = −55 °C; (▲) T_p = 0 °C.

Table IX
Comparison of Properties of the Anisotactic Polypropylenes Obtained with the δ-$TiCl_3$/$AlEt_2Cl$ and *rac*-Et[Ind]$_2$ZrCl/MAO Systems

	T_m, °C		X_c, %		[*mmmm*]	
fraction	Zr[a]	Ti[b]	Zr[a]	Ti[b]	Zr[a]	Ti[b]
C_{7i}		168		67–68		0.95
T_p = −55 °C	154		68		0.92	
T_p = 0 °C	144		68		0.89	
C_7		143		47		0.76
T_p = −55 °C	139		65		0.79	
T_p = 0 °C	140		48		0.82	
C_6, T_p = 70 °C	113	134.5	59	39	0.67	0.64
C_5, T_p = 70 °C	105	115	54	28	0.62	0.44

[a] *rac*-Et[Ind]$_2$$ZrCl_2$/MAO. [b] δ-$TiCl_3$/$AlEt_2Cl$.[34b]

from the β-methylene group produces an internal olefin of VI which is not polymerized by ZN catalyst.

Small amounts of ethylene impurity in the monomer had been suggested to explain the presence of the tetramethylenes in PP. However, the processes would have to involve a sequence of 1,2 propene insertion, ethylene insertion, and 2,1 propene insertion in order to form the sequence V.

The presence of tetramethylene sequence indicates that secondary insertion occurred to a small extent under certain

Scheme I
Processes Leading to "1,3-Enchainment"

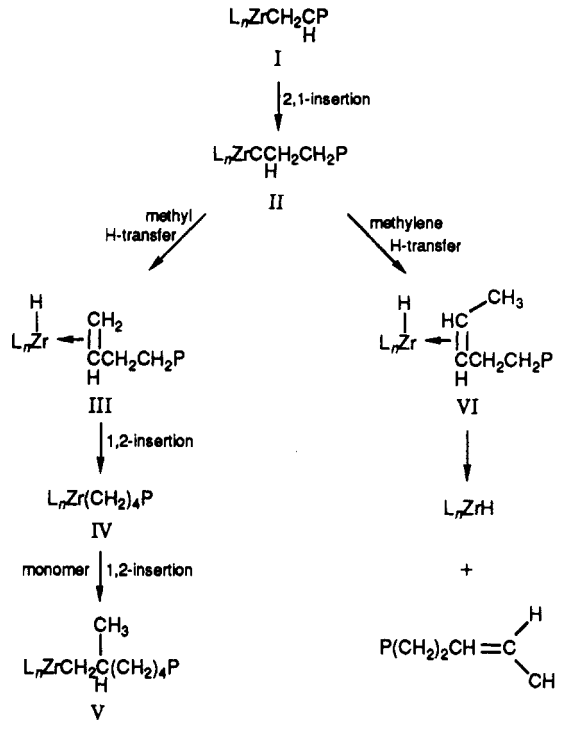

conditions. Products containing this regiochemical error are found mainly in the ether and acetone fractions.

At a low Al/Zr ratio there are found tail to tail units in the PP chain. Peaks 7 and 8 in Figure 12 are erythro methyl carbons and the adjacent peaks are due to the threo methyl carbons. Therefore, the insertion is not highly regiospecific at a low Al/Zr ratio for the Et[Ind]$_2$ZrCl$_2$ system. Apparently, large amounts of MAO are required for both regiospecificity and stereoselectivity.

Conclusions

Kaminsky and co-workers[13] reported that Et[Ind]$_2$ZrCl$_2$/MAO and Et[IndH$_4$]$_2$ZrCl$_2$/MAO catalysts produced only isotactic PP, but the ^{13}C NMR isotacticity indices are not high and the polymers were not fractionated properly. This has been found to be untrue in this work and by others[20] for the former catalyst and with the latter system as well.[41] In fact we have demonstrated that the stereospecificity of the group IV metallocene/MAO catalyst is very dependent on T_p, the [Al]/[Zr] ratio, and other experimental conditions. In the case of the Et[IndH$_4$]$_2$ZrCl$_2$/MAO we found[41] that the PP obtained at T_p = 30 °C and [Al]/[Zr] = 3200 is all soluble in *n*-heptane and has [*mmmm*] = 0.90 and T_m = 132.3 °C. The same catalyst at T_p = −15 °C and [Al]/[Zr] = 2700 gave PP, which is 58% insoluble in refluxing *n*-heptane, [*mmmm*] = 0.98, and T_m = 152.4 °C.[42] Under any experimental conditions, these catalysts have lower stereochemical and regiochemical controls than the heterogeneous ZN catalysts. The degree of control decreases greatly with the increase of T_p and the decrease of the Al/Zr ratio, as indicated by the T_m of the polymer and its homosteric sequence distribution. These anisotactic PPs exhibit a distinct propensity for crystallization in the γ-modification, which was not transformed to the α-modification upon heating. It is proposed that the anisotactic PP chains contain inversion of helical configuration and direction via a TT conformation probably due to non-self-correcting single *r* insertion error. The ^{13}C NMR data will be analyzed for the statistical sequence distribution to shed light on the mechanism of chain propagation. In fact, the microstructure of the polymer is a record of changes in stereochemical control of the *ansa*-metallocene complex.

Acknowledgment is made to the donors of the Petroleum Research Fund, administered by the American Chemical Society, in support of this research. B.R. was supported by a BASF postdoctoral fellowship. Assistance by BASF in performing intrinsic viscosity, GPC, light scattering, and some of the NMR spectroscopic measurements is also acknowledged. Professor T. Atkins checked our X-ray results and proposed the usage of the prefix "an" in describing polymers with low stereoregularity. Acknowledgment is also made to Professor W. Kaminsky for a sample of *rac*-Et[Ind$_2$]ZrCl$_2$ and the synthesis procedure for MAO.

References and Notes

(1) A preliminary report of this work can be found in: Rieger, B.; Chien, J. C. W. *Polym. Bull.* **1989**, *21*, 1159.
(2) For an account of the development of the MgCl$_2$-supported catalysts, see: (a) Galli, P.; Milani, M.; Simonazzi, T. *Polym. J.* **1985**, *17*, 1. (b) Galli, P.; Luciani, L.; Cecchin, G. *Angew. Makromol. Chem.* **1981**, *94*, 63.
(3) The preparation of a supported catalyst from crystalline MgCl$_2$ was described by: (a) Chien, J. C. W.; Wu, J. C.; Kuo, C. I. *J. Polym. Sci., Polym. Chem. Ed.* **1982**, *20*, 2019. The preparation of a higher activity catalyst from soluble MgCl$_2$ alcoholates is given in ref 3b. (b) Hu, Y.; Chien, J. C. W. *J. Polym. Sci., Part A* **1988**, *26*, 2003.
(4) Comparisons of [C*] and k_p of various catalysts have been made. For ethylene polymerization: (a) Reichert, K. H. *Angew. Makromol. Chem.* **1981**, *94*, 1. For propylene polymerization: (b) Chien, J. C. W.; Hu, Y. *J. Polym. Sci., Part A* **1988**, *26*, 2973. (c) Chien, J. C. W.; Hu, Y.; Vizzini, J. C. *J. Polym. Sci., Part A*, in press.
(5) The effects of electron-donating promoters had been discussed. For ethylene polymerization: (a) Chien, J. C. W.; Bres. P. *J. Polym. Sci., Polym. Chem. Ed.* **1986**, *24*, 1967, 2483. For propylene polymerization by c-MgCl$_2$/TiCl$_3$ catalysts: (b) Chien, J. C. W.; Hu, Y. *J. Polym. Sci., Polym. Chem. Ed.* **1987**, *25*, 2847, 2881. For propylene polymerization by s-MgCl$_2$/TiCl$_3$ catalysts: refs 3b and 4c.
(6) (a) Breslow, D. S.; Newburg, N. R. *J. Am. Chem. Soc.* **1957**, *79*, 5072. (b) Natta, G.; Pino, P.; Mazzanti, G.; Giannini, V. *J. Am. Chem. Soc.* **1957**, *79*, 2975.
(7) Chien, J. C. W. *J. Am. Chem. Soc.* **1959**, *81*, 86.
(8) Reichert, K. H.; Meyer, K. R. *Makromol. Chem.* **1973**, *169*, 163.
(9) Grogorjan, E. A.; Dyachkovskii, F. S.; Shilov, A. E. *Vysokomol. Soedin.* **1965**, *7*, 145.
(10) (a) Sinn, H.; Kaminsky, W.; Vollmer, H.-J.; Woldt, R. *Angew. Chem.* **1980**, *92*, 396. (b) Sinn, H.; Kaminsky, W. *Adv. Organomet. Chem.* **1980**, *18*, 99. (c) Kaminsky, W.; Miri, M.; Sinn, H.; Woldt, R. *Makromol. Chem., Rapid Commun.* **1983**, *4*, 417.
(11) Pino, P.; Mulhaupt, R. *Angew. Chem., Int. Ed. Engl.* **1980**, *19*, 857.
(12) (a) Wild, F. R. W. P.; Zsolnai, L.; Huttner, G.; Brintzinger, H. H. *J. Organomet. Chem.* **1982**, *232*, 233. (b) Wild, F. R. W. P.; Wasiacionek, M.; Huttner, G.; Brintzinger, H. H. *J. Organomet. Chem.* **1985**, *288*, 63.
(13) (a) Kaminsky, W.; Külper, K.; Brintzinger, H. H.; Wild, F. R. W. P. *Angew. Chem.* **1985**, *97*, 507. (b) Kaminsky, W. *Angew. Makromol. Chem.* **1986**, *145/146*, 149. (c) Kaminsky, W. *Catalytic Polymerization of Olefins*; Keii, T., Soga, K., Eds.; Kodansha Elsevier: Tokyo, 1986; p 293.
(14) Ewen, J. A. *Catalytic Polymerization of Olefins*; Keii, T., Soga, K., Eds.; Kodansha Elsevier: Tokyo, 1986; p 271.
(15) Hanson, K. R. *J. Am. Chem. Soc.* **1966**, *88*, 2731.
(16) Ewen, J. A.; Jones, R. L.; Razavi, A.; Ferrara, J. D. *J. Am. Chem. Soc.* **1988**, *110*, 6256.
(17) Ishihara, N.; Seimiya, T.; Kuramoto, M.; Uoi, M. *Macromolecules* **1986**, *19*, 2465.
(18) Doi, Y.; Suzuki, T.; Keii, T. *Makromol. Chem., Rapid Commun.* **1981**, *2*, 293.
(19) Soga, K.; Shiono, T.; Takemura, S.; Kaminsky, W. *Makromol. Chem., Rapid Commun.* **1987**, *8*, 305.
(20) (a) Grassi, A.; Zambelli, A.; Resconi, L.; Albizzati, E.; Mazzochi, R. *Macromolecules* **1988**, *21*, 617. (b) Cheng, H. N.; Ewen, J. A. *Makromol. Chem.* **1989**, *190*, 1931.

(21) Gaylord, N. G.; Mark, H. M. *Linear and Stereoregular Addition of Polymers*; Interscience: New York, 1959.
(22) Natta, G. *J. Polym. Sci.* **1959**, *34*, 531.
(23) Pasquon, I. *Pure Appl. Chem.* **1967**, *15*, 465.
(24) The three limiting stereochemical structures for polypropylenes are atactic, isotactic, and syndiotactic. Atactic polymer is amorphous (0% crystallinity) has $mm = rr = 0.25$ and $mr = 0.5$ such as the *n*-pentane-soluble fraction of the polymers obtained with β-$TiCl_3$/$AlEt_2Cl$ at 15 °C (Wolfsgruber, C.; Zannoni, G.; Rigamonti, E.; Zambelli, A. *Makromol. Chem.* **1975**, *176*, 2765) and with VCl_3/$AlEt_2Cl$ at 15 °C (Doi, Y.; Suzuki, E.; Kei, T. *Makromol. Chem., Rapid Commun.* **1981**, *2*, 293). The isotactic polypropylene should be insoluble in trichlorobenzene and has $T_m = 176$ °C and 75–85% crystallinity.[18] However, by common practice the polymer insoluble in *n*-heptane, with $T_m \geq 165$ °C, $mm > 0.95$, and 67–68% crystallinity, is accepted as isotactic polypropylene. To describe the polypropylenes obtained with the metallocene/MAO catalysts as poorly isotactic or low in isotacticity is insufficiently informative. Prof. T. Atkins and J. Atkins of the Bristol University deemed the Greek prefix "an" to be the most appropriate one to describe structures that deviate away from the limiting structures. Rieger, B.; Chien, J. C. W. *Polym. Bull.* **1989**, *21*, 159. This has the advantage of being applicable to both anisotactic ($T_m < 165$ °C, $[m^n] > [r^n]$) and ansyndiotactic ($T_m < 184$ °C, $[r^n] > [m^n]$). We are aware that this prefix has been used previously by G. Natta and P. Corradini (*Atti. Accad. Naz. Lincei, Mem. Cl. Sci. Fis., Mat. Natl., Sez. II* **1955**, *4*, 73) to mean polymers having an equal number of *randomly* distributed substituents on both sides of the chain, but this usage has not taken hold because of rare occurrence.
(25) Kaminsky, W.; Hähnsen, H. U.S. Patent 4544762, 1985.
(26) (a) Chien, J. C. W.; Wang, B. P. *J. Polym. Sci., Part A* **1988**, *26*, 3089. (b) Chien, J. C. W.; Wang, B. P. *J. Polym. Sci., Part A* **1990**, *28*, 15.
(27) (a) Natta, G. *J. Polym. Sci.* **1955**, *16*, 143. (b) Natta, G.; Pino, P.; Mazzanti, G. *Gazz. Chim. Ital.* **1957**, *87*, 528.
(28) Wang, B. P. Ph.D. Dissertation, University of Massachusetts, Amherst, MA, 1988.
(29) Ewen, J. A. *J. Am. Chem. Soc.* **1984**, *106*, 6355.
(30) Chien, J. C. W.; Rieger, B.; Herzog, H. M. *J. Polym. Sci., Part A*, in press.
(31) (a) Natta, G.; Pino, P.; Corradini, P.; Danusso, F.; Mantica, E.; Mazzanti, G.; Moraglio, G. *J. Am. Chem. Soc.* **1955**, *77*, 1708. (b) Natta, G.; Corradini, P. *Nuovo Cimento, Suppl.* **1960**, *15*, 40. (c) Mencik, Z. *J. Macromol. Sci., Phys.* **1972**, *B6*, 101. (d) Hirsaka, M.; Seto, T. *Polym. J.* **1973**, *5*, 111.
(32) Some reports regarding the β-modification of polypropylene and the $\beta \rightarrow \alpha$ transformation are as follows: (a) Keith, H. D.; Padden, F. J. *J. Appl. Phys.* **1959**, *30*, 1485. (b) Forgacs, P.; Tolochko, B. P.; Sheromov, M. A. *Polym. Bull.* **1981**, *6*, 127. (c) Gomez, M. A.; Tanaka, H.; Tonelli, A. J. *Polymer* **1987**, *28*, 2227.
(33) Some reports regarding the γ-modification of polypropylene and the $\gamma \rightarrow \alpha$ transformation are as follows: (a) Pae, K. D.; Morrow, D. R.; Sauer, J. A. *Nature* **1966**, *211*, 514. (b) Kardoss, J.; Christiansen, A. W.; Baer, E. *J. Polym. Sci., Polym. Phys. Ed.* **1966**, *4*, 777. (c) Pae, K. D. *J. Polym. Sci., Polym. Phys. Ed.* **1968**, *6*, 657. (d) Lotz, B.; Graff, S.; Wittmann, J. C. *J. Polym. Sci., Polym. Phys.* **1986**, *24*, 2017. (e) Morrow, D. R.; Newman, B. Z. *J. Appl. Phys.* **1968**, *39*, 4944. (f) Krestev, V. P.; Dobreva, B.; Atanasov, A. M.; Nedkov, E. T. *Morphology Polymers*, W. de Gruyter & Co.: Berlin, 1986; p 303. (g) Addink, E. J.; Beintema, J. *Polymer* **1961**, *2*, 185. (h) Turner-Jones, A.; Aizlewood, J. M.; Beckett, D. R. *Makromol. Chem.* **1964**, *75*, 134. (i) Corradini, P.; Petraccone, V.; Pirozzi, B. *Eur. Polym. J.* **1983**, *19*, 249. (j) Kojima, M. *J. Polym. Sci., Polym. Phys. Ed.* **1968**, *6*, 1255.
(34) (a) Chien, J. C. W. *J. Polym. Sci., Part A* **1963**, *1*, 425, 1839. (b) Keii, T. *Kinetics of Ziegler-Natta Polymerization*; Kodauska: Tokyo, 1972.
(35) Chien, J. C. W. *J. Polym. Sci., Polym. Chem. Ed.* **1963**, *1*, 425.
(36) Flory, P. J. *Principles of Polymer Chemistry*; Cornell University Press: Ithaca, NY, 1953; p 568.
(37) Danusso, F.; Gianotti, G. *Eur. Polym. J.* **1968**, *4*, 165.
(38) (a) Natta, G. *Soc. Plast. Eng.* **1959**, *15*, 373. (b) Combs, R. L.; Slonaker, D. F.; Joyner, F. B.; Coover, H. W. *J. Polym. Sci., Polym. Chem. Ed.* **1967**, *5*, 215.
(39) Corradini, P.; Allegra, G. *Atti. Accad. Naz. Lincei, Cl. Sci. Fis., Mat. Nat., Rend.* **1961**, *30*, 516.
(40) Pino, P. In *Integration of Fundamental Polymer Science and Technology*; Kleintjens, L. A., Lewiston, P. J., Eds.; Elsevier: New York, 1988.
(41) Chien, J. C. W.; Sugimoto, R., submitted for publication in *J. Polym. Sci. Part A*.
(42) Tsutsui, T.; Mizuno, A.; Kashiwa, N. *Makromol. Chem.* **1989**, *190*, 1177.

Registry No. *rac*-Et[Ind]$_2$ZrCl$_2$, 100080-82-8; propylene, 115-07-1; polypropene, 9003-07-0.

Forced Rayleigh Scattering on a Soluble Conducting Polymer

Daniel R. Spiegel*

Department of Physics and Institute for Polymers and Organic Solids, University of California, Santa Barbara, Santa Barbara, California 93106

Received September 26, 1989; Revised Manuscript Received January 23, 1990

ABSTRACT: Forced Rayleigh scattering (FRS) is used to probe the dynamics of a conducting polymer, poly(3-octylthiophene), in solution. The optical labels employed are photoexcited states on the chains themselves; chemical addition of a photochromic labeling attachment is not required. The main feature of the time dependence of the diffracted intensity is an exponential time decay; from the quadratic dependence of the decay time on the grating wave vector, we find a translational diffusion coefficient in the dilute regime of $(8 \pm 1) \times 10^{-8}$ cm^2/s, corresponding to a hydrodynamic radius of $R_h = 130 \pm 15$ Å. It is shown that the mean value measured in the experiments is the *z*-average diffusion coefficient, in contrast with FRS experiments in which photochromic labels are chemically attached to the ends of the chains. We propose that bipolarons are the excited states responsible for chain labeling, based in part on the photoinduced absorption spectra for poly(3-alkylthiophenes).

Introduction

The technique of forced Rayleigh scattering (FRS), which has alternatively been called holographic grating relaxation spectroscopy and the holographic grating technique,[1-4] has proved to be a powerful tool in the measurement of the diffusive dynamics of condensed phases. The experiment employs an optical pump-and-probe technique: Two coherent, absorbed laser beams (the pump beams) are used to form interference fringes within a sample, resulting in a spatially periodic excited-state

* Permanent address: Enrico Fermi Institute, University of Chicago, Chicago, IL 60637.

0024-9297/90/2223-3568$02.50/0